Article

A Stochastic Bayesian Neural Network for the Mosquito Dispersal Mathematical System

Suthep Suantai [1,2], Zulqurnain Sabir [3], Muhammad Asif Zahoor Raja [4] and Watcharaporn Cholamjiak [5,*]

1 Research Group in Mathematics and Applied Mathematics, Faculty of Science, Chiang Mai University, Chiang Mai 50200, Thailand
2 Data Science Research Center, Department of Mathematics, Faculty of Science, Chiang Mai University, Chiang Mai 50200, Thailand
3 Department of Mathematics and Statistics, Hazara University, Mansehra 21300, Pakistan
4 Future Technology Research Center, National Yunlin University of Science and Technology, 123 University Road, Section 3, Yunlin, Douliou 64002, Taiwan
5 School of Science, University of Phayao, Phayao 56000, Thailand
* Correspondence: watcharaporn.ch@up.ac.th

Abstract: The objective of this study is to examine numerical evaluations of the mosquito dispersal mathematical system (MDMS) in a heterogeneous atmosphere through artificial intelligence (AI) techniques via Bayesian regularization neural networks (BSR-NNs). The MDMS is constructed with six classes, i.e., eggs, larvae, pupae, host, resting mosquito, and ovipositional site densities-based ODEs system. The computing BSR-NNs scheme is applied for three different performances using the data of training, testing and verification, which is divided as 75%, 15%, 10% with twelve hidden neurons. The result comparisons are provided to check the authenticity of the designed AI method portrayed by the BSR-NNs. The AI based BSR-NNs procedure is executed to reduce the mean square error (MSE) for the MDMS. The achieved performances are also presented to validate the efficiency of BSR-NNs scheme using the process of MSE, correlation, error histograms and regression.

1. Introduction

The spread of the mosquito has a significant role in supporting the persistence and resurgence of various vector-borne diseases. There are numerous studies made on spatial variability based on mosquitoes, including the human association with vectors, breeding and host locations, the community pattern of mosquitoes, and the capacity to manage the spread of the virus. Floral, dengue, yellow fever, malaria, and other serious viruses are spread through mosquitoes. Malaria represents a significant geographic differential that is primarily affected by social migration, treatment response, and changes in the climate [1,2]. The environment of mosquitoes has a dominant contribution in preventing disease from spreading in the range of 100–1000 m [3]. Like some of the other insects, mosquitos can migrate in just about any direction, but they can also transport partial stocks when supplies are readily available.

Ronald Ross initially addressed the need to manage and prevent the spread of vector-borne diseases a century back [4]. Additionally, he noted that the public health-based community does not address this issue. According to Ross, the ratios of mosquito reproduction, immigration, mortality, and emigration determine the number of insects in any given region. According to Manga et al. [5], the temporal difference in the mosquitoes' usage of different characteristics affects both their reproductive rate and dispersal. This demonstrates the discrepancy in vector density, host knowledge, and disease transmission capacity [6,7]. The characteristics of the sources on the transmission may not make

sense, for example, the presence of inactive larval habitats may indicate high bite densities [8]. Experiments on mosquito transmission, meanwhile, provide some encouraging results [9,10].

The outcomes of occurrences that are motivating to a wide range of fields are often provided and understood by mathematical techniques, but insufficient systems possess integrated diversity or dispersal features of a close population vector [11–13]. The insect's adult stages have been divided into a number of categories [14]. A system can include the architecture of the mosquito life cycle, distribution/feeding cycle, spatial variation for the insect species, and propagation/diversity impacts. The diffusion technique, which simulates space as just a persisting variable, has generally been utilized in space studies. Despite the validity of distribution networks that took heterogeneity into consideration, integrating a number of distracting aspects is difficult [15,16]. A metapopulational method is more suitable for modeling mosquito dispersion in zones that are discontinuous squares, and the population is allotted to isolated regions. At each point, the population is divided into subgroups that correlate to various scenarios and various categorized systems. The diversity present in the habitats of the spreading disease has been harmonized by a number of dispersion frameworks [17,18]. Furthermore, the aqueous portions of mosquitoes offer a complete context to represent the non-uniform schemes of the insects' interference management.

The mosquito dispersal mathematical system (MDMS) in a heterogeneous atmosphere is classified into six densities: eggs $E(u)$, larvae $L(u)$, pupae $P(u)$, host density $A_h(u)$, resting mosquito $A_r(\xi)$, and ovipositional site $A_0(u)$, presented in Figure 1.
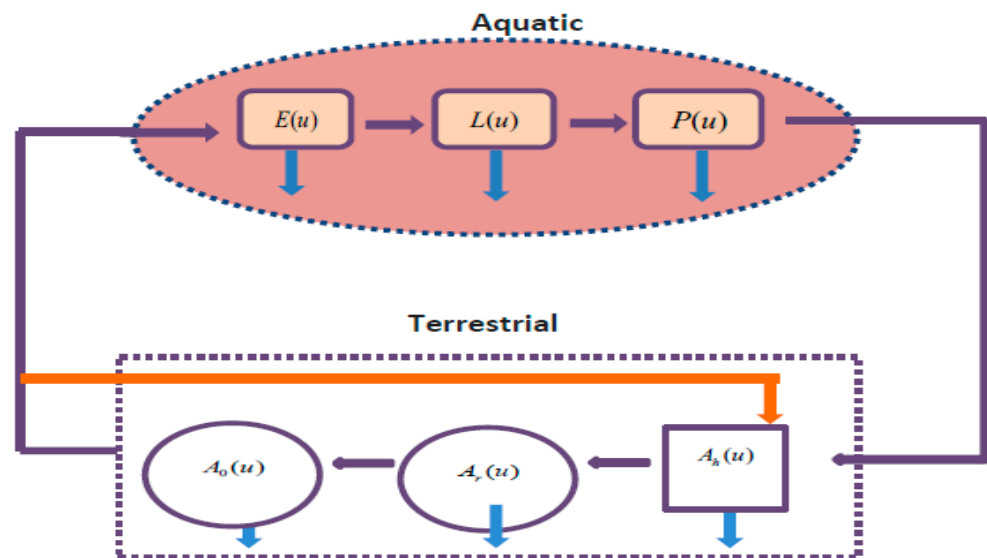
Figure 1. Schematic illustrations of MDMS based on the densities of eggs $E(u)$, larvae $L(u)$, pupae $P(u)$, host $A_h(u)$, resting mosquito $A_r(\xi)$ and ovipositional site $A_0(u)$.

The mathematical form of the MDMS is given as [19]:

$$\begin{cases} \frac{d}{du}E(u) = b\rho_{A_0}A_0(u) - (\rho_E + \mu_E)E(u), & E_0 = I_1, \\ \frac{d}{du}L(u) = \rho_E E(u) - (\rho_L + \mu_{L_2}L(u) + \mu_{L_1})L(u), & L_0 = I_2, \\ \frac{d}{du}P(u) = \rho_L L(u) - (\mu_P + \rho_P)P(u), & P_0 = I_3, \\ \frac{d}{du}A_h(u) = \rho_{A_0}A_0(u) - (\mu_{A_h} + \rho_{A_h})A_h(u) + \rho_P P(u), & (A_h)_0 = I_4, \\ \frac{d}{du}A_r(u) = -(\rho_{A_r} + \mu_{A_r})A_r(u) + \rho_{A_h}A_h(u), & (A_r)_0 = I_5, \\ \frac{d}{du}A_0(u) = \rho_{A_r}A_r(u) - (\mu_{A_0} + \rho_{A_0})A_0(u), & (A_0)_0 = I_6. \end{cases} \tag{1}$$

The dynamics behaviour of MDMS represented with in six classes, i.e., eggs, larvae, pupae, host, resting mosquito and ovipositional site densities-based ODE system, while the initial conditions are I_1 to I_6 represented the start values of the six classes, respectively. The

global and local stability of the system is performed in [19] and after theoretical convergence proofs following set of the parameters for MDMS are chosen as shown in Table 1 [19].

Table 1. Suitable Values for the MDMS.

Index	Particulars	Values	Range
ρ_{A_r}	Resting mortality rate (MR) to go in ovipositional places	0.5	0.30–0.56
μ_P	Pupae MR	0.4	0.22–0.52
μ_E	MR of eggs	0.5	0.32–0.8
ρ_L	Mature larvae rate into pupae	0.12	0.08–0.17
μ_{Ar}	Resting MR mosquitoes	0.0043	0.03–0.01
ρ_{Ah}	Host mosquitos using the latent conditions	0.46	0.322–0.6
μ_{L2}	Dependent density rate-based larvae mortality	0.02	0–1
b	Female eggs located per ovipositional	60	50–300
μ_{L1}	Density-independent based larvae MR	0.4	0.30–0.58
μ_{A0}	MR Mosquito using the ovipositional sites	0.41	0.41–0.56
ρ_P	Rate of pupae growth into mature	0.7	0.33–1
ρ_{A0}	Ovipositional rate	3.2	3–4
μ_{Ah}	Mosquitoes MR using the hosts penetrating	0.18	0.12–0.23
ρ_E	Eggs rate into larvae	0.4	0.33–1

The motive of these investigations is to examine the numerical evaluations based on the mosquito dispersal mathematical system (MDMS) in a heterogeneous atmosphere using the artificial intelligence (AI) procedures enhanced by the Bayesian regularization neural networks (BSR-NNs). The AI-based stochastic solvers have been used to solve various stiff natured models [20–27], however, the MDMS has not been solved before using the BSR-NNs. Recently, the stochastic applications have been applied in various systems, some of them are SITR models, singular models, periodic differential systems, dengue fever model, food chain models and prediction/delay/pantograph systems please see reference [28–30] and citations mentioned therein. The authors were inspired through these well-known applications to propose a consistent, reliable and robust platform to solve the MDMS by applying the BSR-NNs. Several notable findings have important implications in the current piece of research are marked as:

- A computational novel AI based BSR-NNs is presented to get the numerical solutions of the MDMS.
- The performance of the AI based BSR-NNs is observed to solve three different variations of the MDMS.
- For the correctness of the AI scheme portrayed by the BSR-NNs, the comparison performances using the obtained and reference solutions have been presented.
- Twelve number of hidden neurons have been taken to solve effectively the MDMS by applying the BSR-NNs.
- The absolute error (AE) is achieved in exceptional performances that demonstrate the accuracy of the BSR-NNs.
- For the solution of the dynamical MDMS, the correlation performances, error histograms, regression are also provided that endorsed the accuracy.

The remaining parts of this study are given as: Section 2 shows the solutions of the MDMS by applying the BSR-NNs. Section 3 presents the numerical solutions of the model. The conclusions are shown in the last Section.

2. Methodology

In this section, the AI scheme enhanced by the BSR-NNs has been presented by using the MDMS with the obligatory descriptions of the scheme along with its implementation procedures.

In order to build the network statistics, the numerical capabilities are enabled using the standard application setting. The computing BSR-NNs scheme is applied for three different performances using the data of training, testing and verification, which is divided

as 75%, 15%, 10% with twelve hidden neurons. For the solution of the MDMS, the optimal cooperation using the matrices with overfitting, underfitting stages, complexity and rapid convergence, the AI scheme enhanced by the BSR-NNs has been provided. These mechanisms have also been adapted in response to extensive reproduction, knowledge, care, practice, and slight system network variations. The workflow illustrations of the BSR-NNs scheme for the MDMS are presented in Figure 2.

The AI based BSR-NNs procedure is presented in Figure 3 that shows the general perception based on the single neuron value. BSR-NNs is constructed on the similar pattern of as portrayed in Figure 3 to models the dynamics of MDMS while the activation function of log-sigmoid is incorporated in hidden layers. Table 2 indicates the execution parameters setting of AI computing scheme enhanced by the BSR-NNs through the small disproportion with premature convergence. Subsequently, the numerical investigations with careful consideration have been conducted with parameters as listed Table 2 by the BSR-NNs stochastic scheme for solving the MDMS.

For the numerical solutions of the dynamical MDMS using the BSR-NNs, the layer procedure is processed, as presented in Figure 4. It contains a single input layer vector using 12 hidden numbers of neurons, six outputs for the classes of MDMS and single input layer of grids of inputs. The nftool commands, which is a Matlab (Version: R2019b) built-in procedure, is used along with suitable choices of the hidden neurons, authentication data, testing measures and learning commands based on the construction of the BSR-NNs solver. The selection of the appropriate for the BSR-NNs is carried out on the basis of extensive simulations/experimentation on the basis of the trade-off between the underfitting, i.e., premature convergence, and overfitting, i.e., greater complexity, scenarios. So, by decreasing number of the neurons to less than 12 we have more chances of underfitting while increasing the number of neurons to greater than 12 gives a slight improvement in accuracy/precision but at the cost of considerable additional computations. Moreover, optimal architecture of neural networks and parameter settings is provided in Figure 4 and Table 2 while small changes with respect to different cases of MDMS has been done during different test experiments in the presented study.

Table 2. Parameter Measures Using the Stochastic Procedure.

Parameter	Settings
Maximum epochs	200
Fitness	0
Hidden neurons	12
Setting up Mu	0.25
Increasing performances of Mu	14
Adaptive Mu performances	6×10^{-2}
Validation fail amount	8
Highest mu values	10^9
Minimum values of gradient	10^{-8}
Train data	75%
Verification statics	10%
Test performances	15%
Sample selection	Random
Output/input/hidden values	Single
Dataset generation	Runge-Kutta
Other	Default

Figure 2. Workflow illustrations of the BSR-NNs scheme for the MDMS.
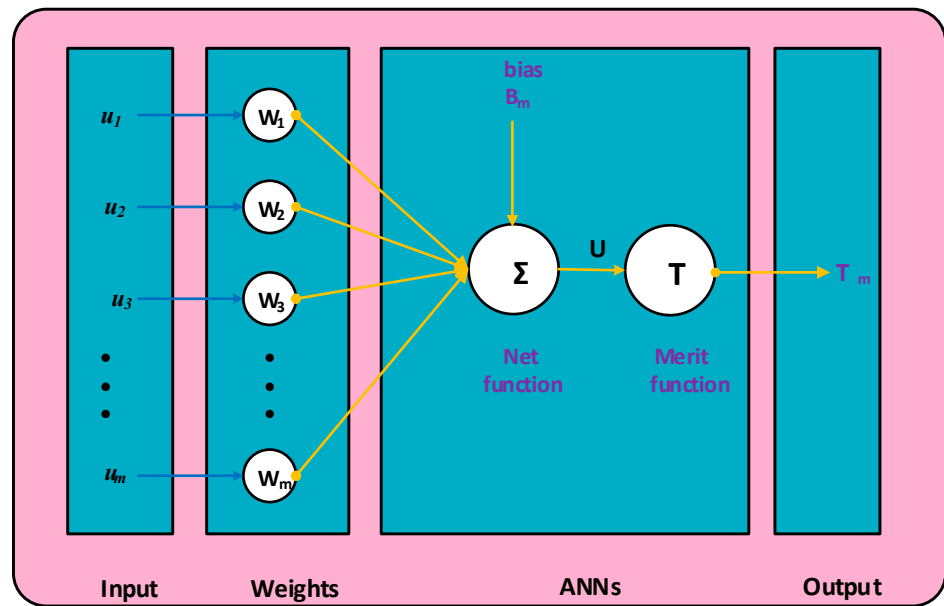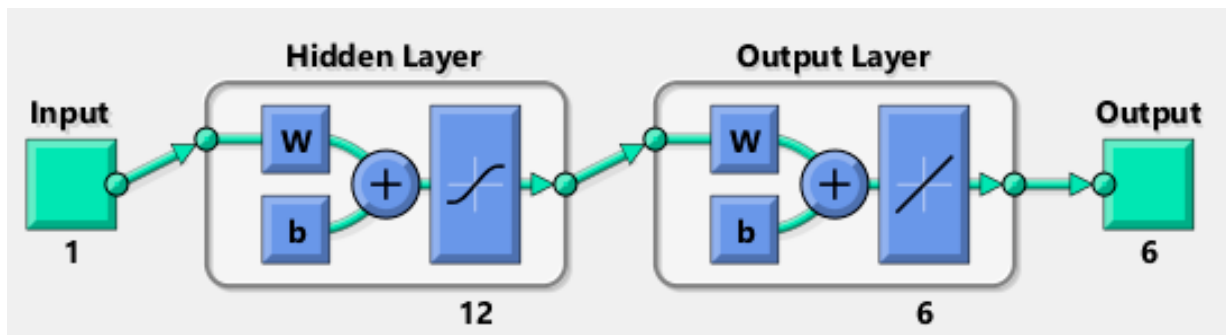
Figure 3. A single layer network.

Figure 4. Proposed BSR-NNs operator for the MDMS.

3. Results and Discussion

The present section shows the numerical results for three variations to solve the MDMS based on reported study [19] by applying the BSR-NNs, presented as:

Case 1: Suppose the MDMS is presented as:

$$
\begin{cases}
\frac{d}{du}E(u) = 192A_0(u) - 0.9E(u), & E_0 = 1 \times 10^{-5}, \\
\frac{d}{du}L(u) = 0.4E(u) - (0.52 + 0.02L(u))L(u), & L_0 = 1 \times 10^{-5}, \\
\frac{d}{du}P(u) = 0.12L(u) - 1.11P(u), & P_0 = 3 \times 10^{-4}, \\
\frac{d}{du}A_h(u) = 3.2A_0(u) - 0.64A_h(u) + 0.7P(u), & (A_h)_0 = 1 \times 10^{-4}, \\
\frac{d}{du}A_r(u) = -0.5043A_r(u) + 0.46A_h(u), & (A_r)_0 = 1 \times 10^{-5}, \\
\frac{d}{du}A_0(u) = 0.5A_r(u) - 3.61A_0(u), & (A_0)_0 = 3 \times 10^{-4}.
\end{cases}
\tag{2}
$$

Case 2: Suppose the MDMS is presented as:

$$\begin{cases} \frac{d}{du}E(u) = 192A_0(u) - 0.9E(u), & E_0 = 3 \times 10^{-5}, \\ \frac{d}{du}L(u) = 0.4E(u) - (0.52 + 0.02L(u))L(u), & L_0 = 3 \times 10^{-5}, \\ \frac{d}{du}P(u) = 0.12L(u) - 1.11P(u), & P_0 = 6 \times 10^{-4}, \\ \frac{d}{du}A_h(u) = 3.2A_0(u) - 0.64A_h(u) + 0.7P(u), & (A_h)_0 = 3 \times 10^{-4}, \\ \frac{d}{du}A_r(u) = -0.5043A_r(u) + 0.46A_h(u), & (A_r)_0 = 3 \times 10^{-5}, \\ \frac{d}{du}A_0(u) = 0.5A_r(u) - 3.61A_0(u), & (A_0)_0 = 6 \times 10^{-4}. \end{cases} \quad (3)$$

Case 3: Suppose the MDMS is presented as:

$$\begin{cases} \frac{d}{du}E(u) = 192A_0(u) - 0.9E(u), & E_0 = 6 \times 10^{-5}, \\ \frac{d}{du}L(u) = 0.4E(u) - (0.52 + 0.02L(u))L(u), & L_0 = 6 \times 10^{-5}, \\ \frac{d}{du}P(u) = 0.12L(u) - 1.11P(u), & P_0 = 9 \times 10^{-4}, \\ \frac{d}{du}A_h(u) = 3.2A_0(u) - 0.64A_h(u) + 0.7P(u), & (A_h)_0 = 6 \times 10^{-4}, \\ \frac{d}{du}A_r(u) = -0.5043A_r(u) + 0.46A_h(u), & (A_r)_0 = 6 \times 10^{-5}, \\ \frac{d}{du}A_0(u) = 0.5A_r(u) - 3.61A_0(u), & (A_0)_0 = 9 \times 10^{-4}. \end{cases} \quad (4)$$

The numerical values presented in equations 2 to 4 are taken in line with the reported study [19] and further detailed for justification of the parameters can be seen in [19]. The solutions have been obtained to solve the MDMS by applying the BSR-NNs using the input [0, 1], with 0.01 step size and 12 numbers of hidden neurons. The achieved numerical measures to solve the MDMS by applying the BSR-NNs are provided in Figure 5 through the MSE and STs. The obtained computing MSE based on the train and test are provided in Figure 5a–c at epochs 3, 5 and 6 for 1st, 2nd and 3rd case performed as 4.9429×10^{-10}, 7.2206×10^{-11} and 3.5449×10^{-11}. Figure 5d–f presents the gradient results, which are given as 5.7431×10^{-8}, 8.9848×10^{-8} and 2.2346×10^{-8}. The predicted data displayed in these plots demonstrates the reliability and consistency of stochastic BSR-NNs for the MDMS. The comparison of the operators using the BSR-NNs for the MDMS are shown in the fitting curves graphs. 6a–c. Figure 6d–f indicates the EHs illustrations that have been provided as -5.8×10^{-6}, -4.7×10^{-7} and 3.51×10^{-7} for 1st to 3rd case. Figure 7 presents the regression performances based on the correlation, which authenticate the correlation is 1 for each variation, which indicates the perfect system. For the MDMS, the statics based on train and test demonstrate the accuracy of the computational stochastic BSR-NNs. Moreover, Table 3 shows the MDMS using the MSE based on the complexity, test, train and generations.
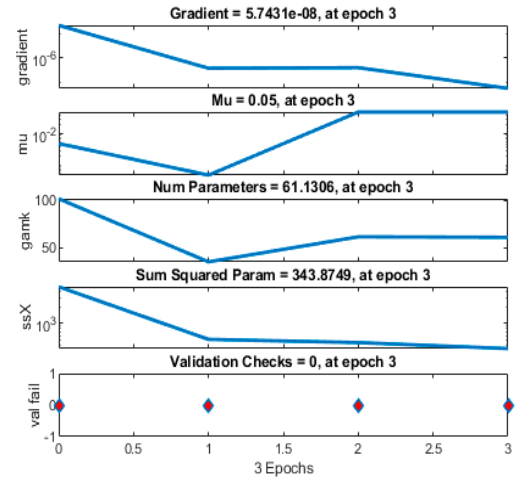
Table 3. ANNs-LMB Procedure to Solve Each Group of the NDMHA.

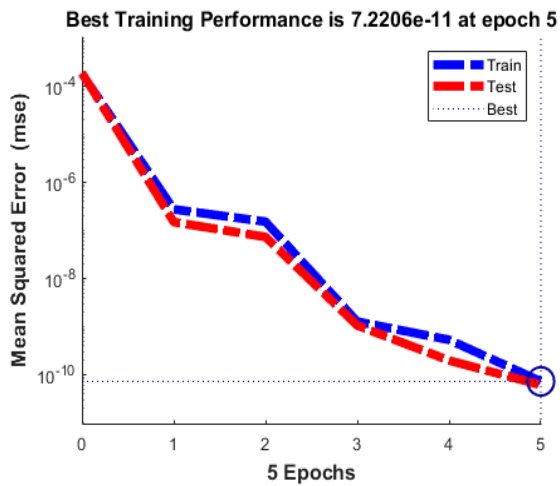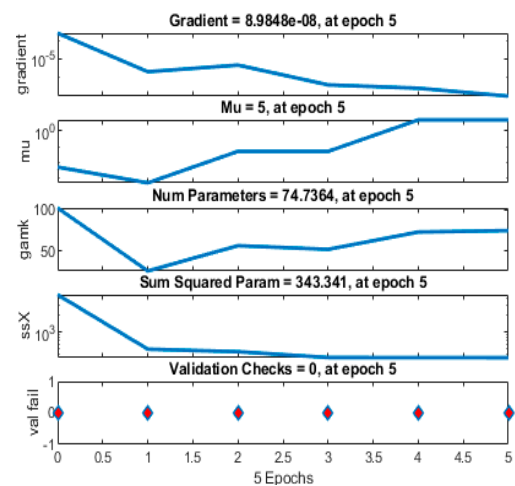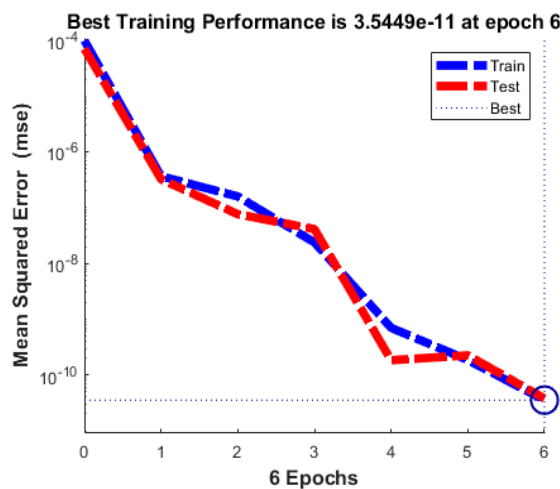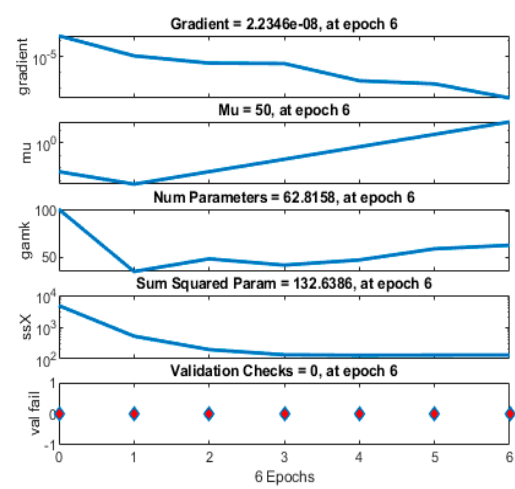| Case	MSE		Epoch	Gradient	Performance	Mu	Time
	Test	Train					
1	5.504×10^{-10}	4.942×10^{-10}	3	5.74×10^{-8}	4.94×10^{-10}	0.0500	4
2	6.064×10^{-11}	7.220×10^{-11}	5	8.98×10^{-8}	7.22×10^{-11}	5	3
3	3.775×10^{-11}	3.544×10^{-11}	6	2.23×10^{-8}	3.54×10^{-11}	50	2
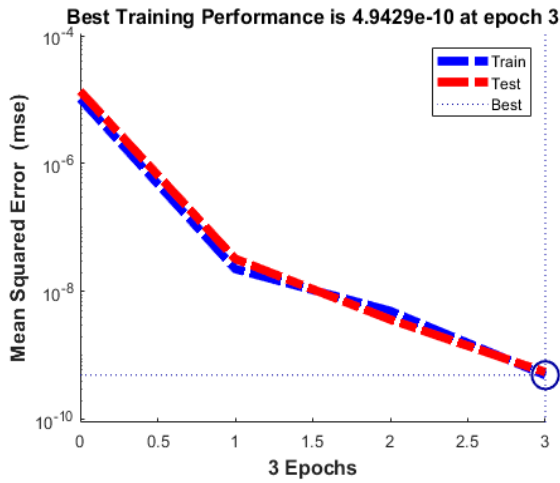
Figure 5. Performances of MSE (**a**–**c**) and STs (**d**–**f**) to solve the MDMS.(**a**) MSE (1); (**b**) MSE (2); (**c**) MSE (3);(**d**) STs (1); (**e**) STs (2); (**f**) STs (3).
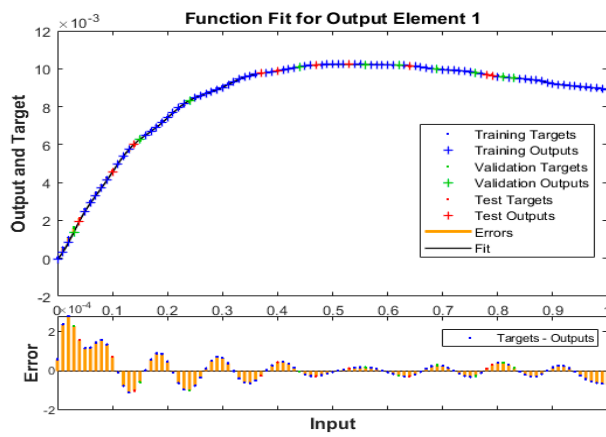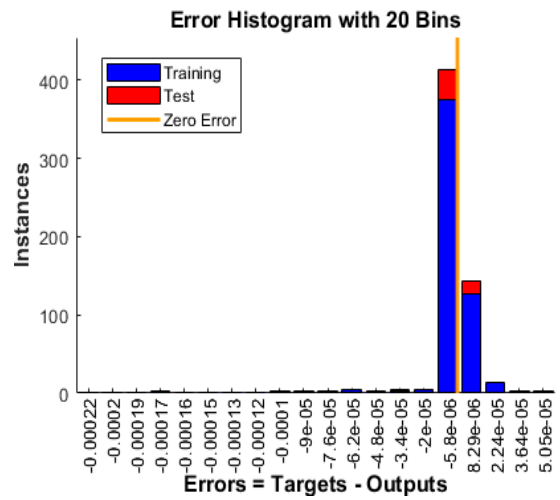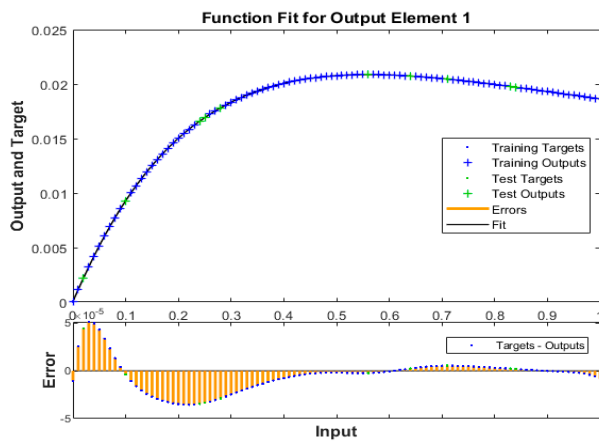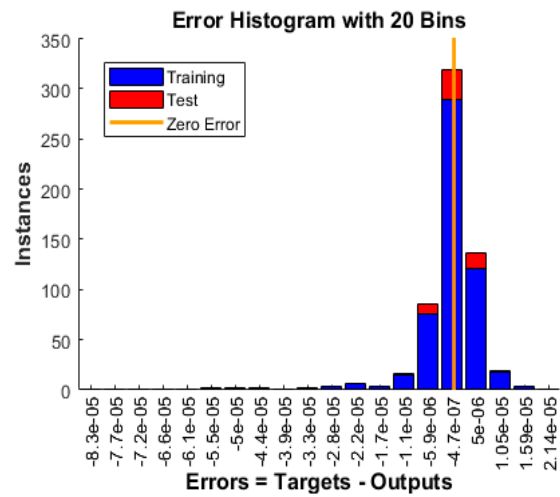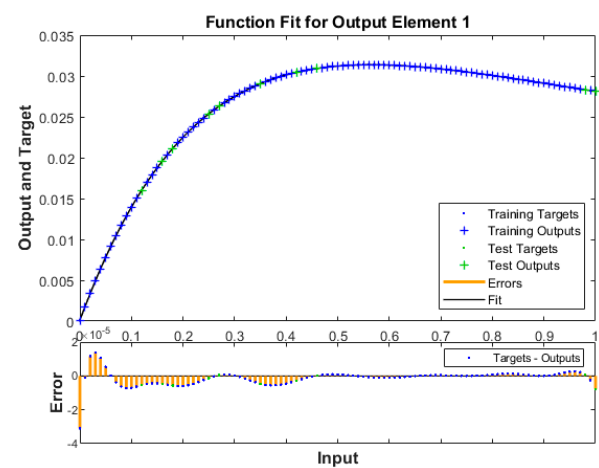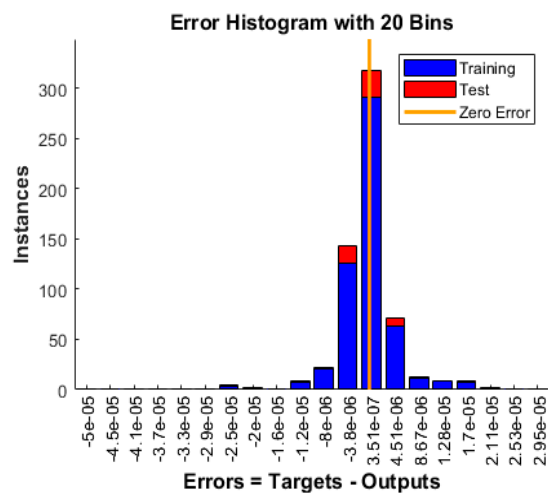
Figure 6. Result outputs and EHs for the MDMS. (**a**) Outputs (1); (**b**) Outputs (2); (**c**) Outputs (3); (**d**) EHs (1); (**e**) EHs (2); (**f**) EHs (3).

(**a**)

(**b**)

(**c**)
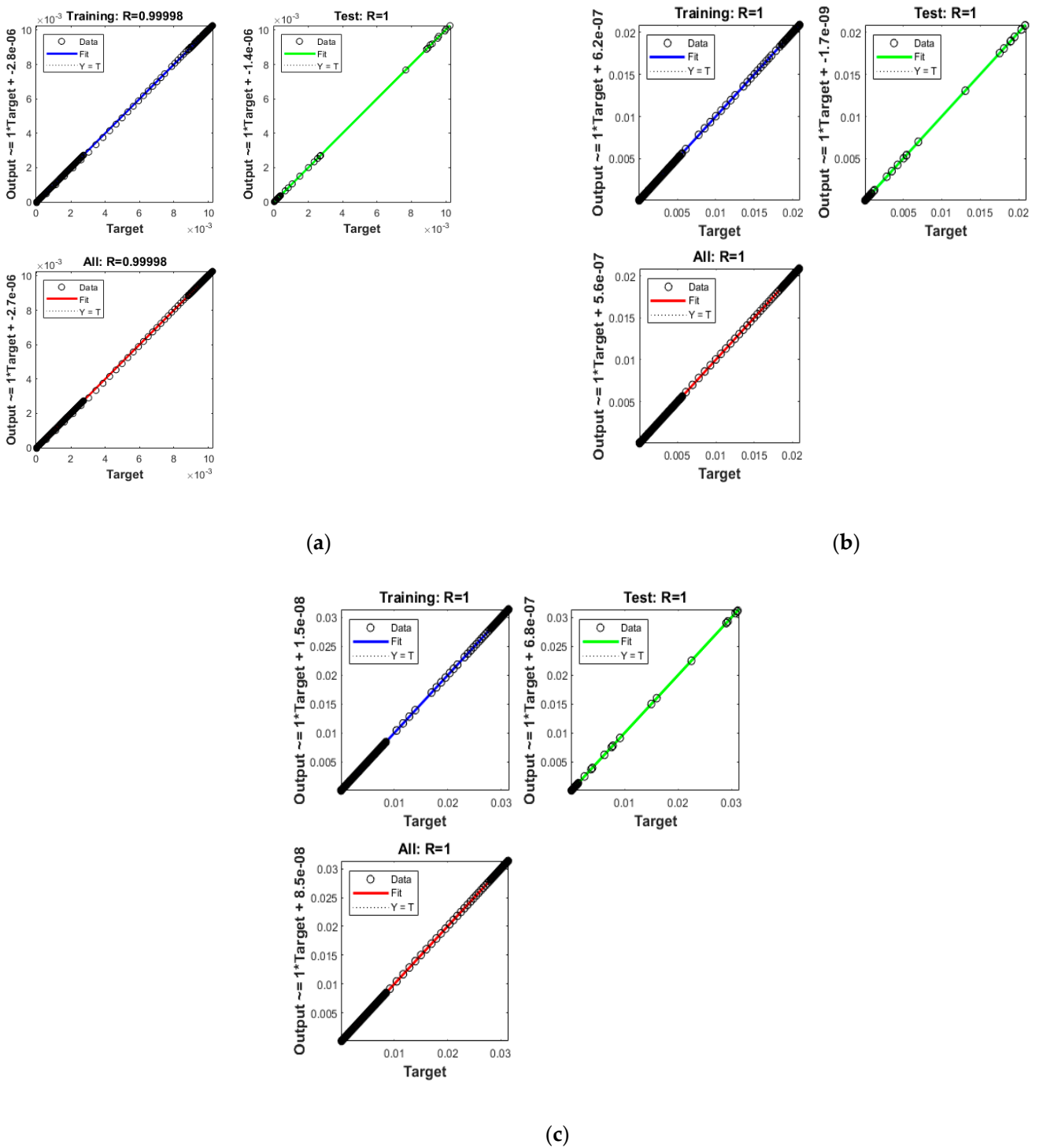
Figure 7. Values of the regression for the MDMS. (**a**) Regression values (1); (**b**) Regression values (2); (**c**) Regression values (3).

Figures 8 and 9 depict the data using the result comparisons and AE measures to solve the MDMS based on BSR-NNs. Figure 8 presents the correctness of the AI scheme together with the BSR-NNs through the comparison of results for solving the MDMS. Figure 9 shows the AE measures for each AI scheme together with the BSR-NNs. The AE for the MDMS based on the density of eggs $E(u)$ lie as 10^{-4}–10^{-5}, 10^{-4}–10^{-6} and 10^{-5}–10^{-6}, larvae $L(u)$ density is shown as 10^{-5}–10^{-6}, 10^{-6}–10^{-7} and 10^{-5}–10^{-7}, density of the pupae $P(u)$ is presented as 10^{-5}–10^{-7}, 10^{-5}–10^{-6} and 10^{-5}–10^{-7}, host density $A_h(u)$ lie

around 10^{-5}–10^{-7}, 10^{-5}–10^{-6} and 10^{-5}–10^{-7}, resting mosquito $A_r(\xi)$ found as 10^{-6}–10^{-7}, 10^{-5}–10^{-6} and 10^{-6}–10^{-7} and ovipositional site $A_0(u)$ shown as 10^{-5}–10^{-7}, 10^{-5}–10^{-6} and 10^{-5}–10^{-7}. These values of the AE present the correctness of AI scheme based on BSR-NNs for solving the MDMS.
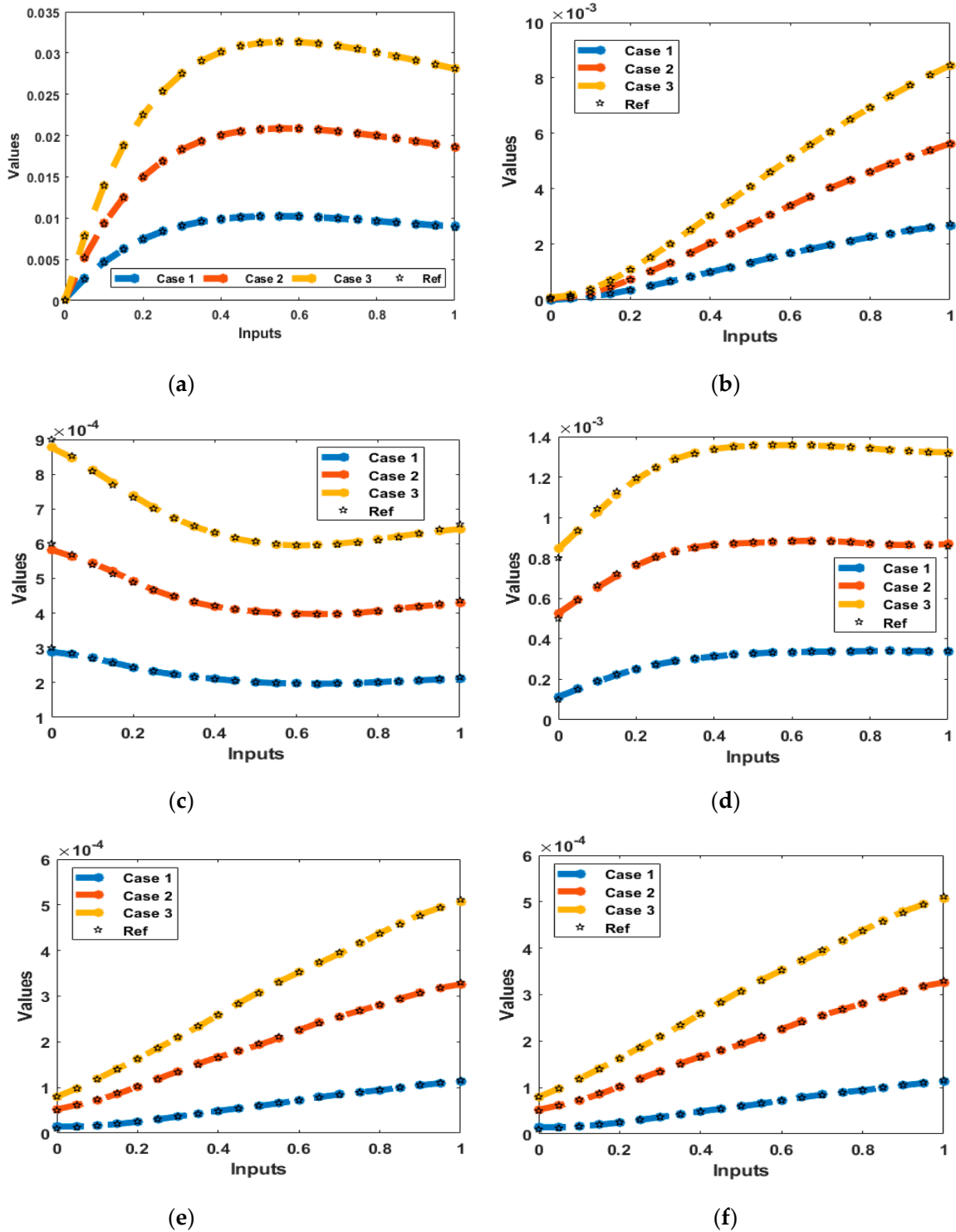
Figure 8. Comparison presentations using the AI based BSR-NNs for solving the MDMS. (**a**) Results: $E(u)$; (**b**) Results: $L(u)$; (**c**) Results: $P(u)$; (**d**) Results: $A_h(u)$; (**e**) Results: $A_r(u)$; (**f**) Results: $A_0(u)$.
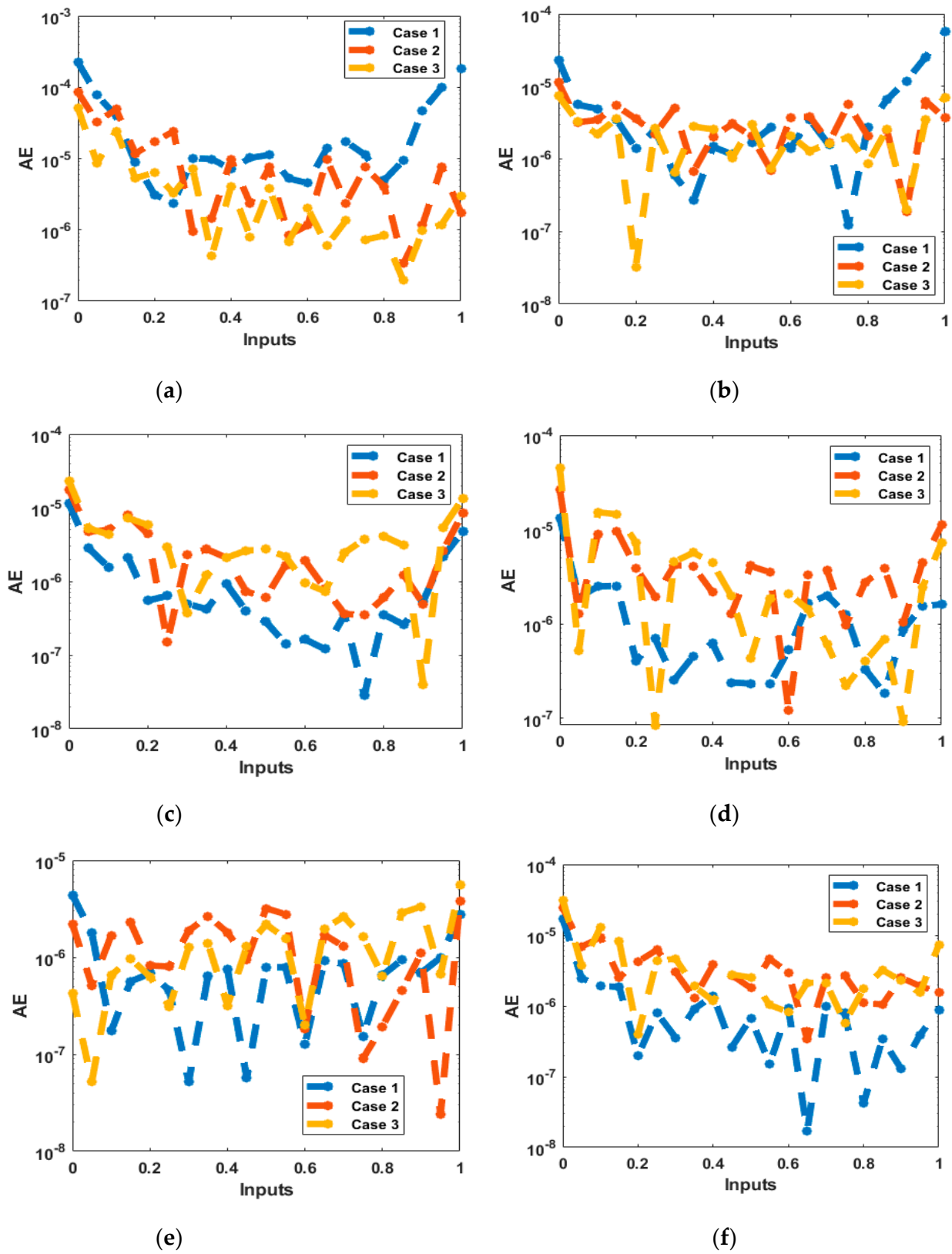
Figure 9. Performances of the AE using the AI based BSR-NNs for solving the MDMS. (**a**) AE: $E(u)$; (**b**) AE: $L(u)$; (**c**) AE: $P(u)$; (**d**) AE: $A_h(u)$; (**e**) AE: $A_r(u)$; (**f**) AE: $A_0(u)$.

4. Concluding Remarks

The purpose of this work is to examine the numerical evaluations of the mosquito dispersal mathematical system in a heterogeneous atmosphere through the procedures of artificial intelligence enhanced by the Bayesian regularization neural networks. The nonlinear differential model has been divided into six classes: eggs, pupae, larvae, host, ovipositional site and resting mosquito densities. Some concluding remarks of the current work are provided as:

- The stochastic artificial intelligence based on Bayesian regularization neural network procedure has never been provided before for the numerical solutions of the MDMS.
- The computing BSR-NNs procedure is implemented to solve three different variations based on the data of training, testing and verification that is respectively given as 75%, 15%, 10%.
- Twelve hidden numbers of neurons have been applied to present the solutions of the nonlinear mathematical system.
- The correctness of the AI based BSR-NNs is observed by using the comparison procedures of the obtained and reference solutions.
- The AE performances in good measures enhance the precision and exactness of the scheme for solving the model.
- The achieved results have been presented to authenticate the efficiency of the artificial intelligence enhanced by the Bayesian regularization neural networks using the regression/correlation, state transitions and error histograms.

In future, the suggested Bayesian regularization based neural network schemes can be applied to present the numerical solutions of the nonlinear and dynamical systems [31–41].

Author Contributions: S.S.; project administration, Z.S.; writing-original draft preparation, M.A.Z.R.; supervision, W.C. writing-review and editing. All authors have read and agreed to the published version of the manuscript.

References

1. Gething, P.W.; Patil, A.P.; Smith, D.L.; Guerra, C.A.; Elyazar, I.R.; Johnston, J.L.; Tatem, A.J.; Hay, S.I. A new world malaria map: Plasmodium falciparum endemicity in 2010. *Malar. J.* **2011**, *10*, 378. [CrossRef] [PubMed]
2. Tatem, A.J.; Rogers, D.J.; Hay, I.S. Estimating the malaria risk of African mosquito movement by air travel. *Malar. J.* **2006**, *5*, 57. [CrossRef] [PubMed]
3. Le Menach, A.; McKenzie, F.E.; Flahault, A.; Smith, D.L. The unexpected importance of mosquito oviposition behaviour for malaria: Non-productive larval habitats can be sources for malaria transmission. *Malar. J.* **2005**, *4*, 23. [CrossRef]
4. Ross, R. An Address on the logical basis of the sanitary policy of mosquito reduction: Delivered at the Section of Preventive Medicine of the International Congress of Arts and Science, Universal Exposition, St. Louis, September, 1904. *Br. Med. J.* **1905**, *1*, 1025. [CrossRef]
5. Manga, L.; Fondjo, E.; Carnevale, P.; Robert, V. Importance of low dispersion of Anopheles gambiae (Diptera: Culicidae) on malaria transmission in hilly towns in south Cameroon. *J. Med. Entomol.* **1993**, *30*, 936–938. [CrossRef]
6. Gu, W.; Novak, R.J. Agent-based modelling of mosquito foraging behaviour for malaria control. *Trans. R. Soc. Trop. Med. Hyg.* **2009**, *103*, 1105–1112. [CrossRef] [PubMed]
7. Cano, J.; Descalzo, M.; Moreno, M.; Chen, Z.; Nzambo, S.; Bobuakasi, L.; Buatiche, J.N.; Ondo, M.; Micha, F.; Benito, A. Spatial variability in the density, distribution and vectorial capacity of anopheline species in a high transmission village (Equatorial Guinea). *Malar. J.* **2006**, *5*, 21. [CrossRef] [PubMed]
8. Ghosh, A.; Chowdhury, N.; Chandra, G. Plant extracts as potential mosquito larvicides. *Indian J. Med. Res.* **2012**, *135*, 581.

9. Gillies, M.T.; Wilkes, T.J. Field experiments with a wind tunnel on the flight speed of some West African mosquitoes (Diptera: Culicidae). *Bull. Entomol. Res.* **1981**, *71*, 65–70. [CrossRef]

10. Midega, J.T.; Mbogo, C.M.; Mwambi, H.; Wilson, M.D.; Ojwang, G.; Mwangangi, J.M.; Nzovu, J.G.; Githure, J.I.; Yan, G.; Beier, J.C. Estimating dispersal and survival of Anopheles gambiae and Anopheles funestus along the Kenyan coast by using mark–release–recapture methods. *J. Med. Entomol.* **2007**, *44*, 923–929. [CrossRef] [PubMed]

11. Ngwa, G.A. On the population dynamics of the malaria vector. *Bull. Math. Biol.* **2006**, *68*, 2161–2189. [CrossRef] [PubMed]

12. White, M.T.; Griffin, J.T.; Churcher, T.S.; Ferguson, N.M.; Basáñez, M.-G.; Ghani, A.C. Modelling the impact of vector control interventions on Anopheles gambiae population dynamics. *Parasites Vectors* **2011**, *4*, 153. [CrossRef] [PubMed]

13. Otero, M.; Solari, H.G.; Schweigmann, N. A stochastic population dynamics model for Aedes aegypti: Formulation and application to a city with temperate climate. *Bull. Math. Biol.* **2006**, *68*, 1945–1974. [CrossRef]

14. Saul, A. Zooprophylaxis or zoopotentiation: The outcome of introducing animals on vector transmission is highly dependent on the mosquito mortality while searching. *Malar. J.* **2003**, *2*, 32. [CrossRef]

15. Raffy, M.; Tran, A. On the dynamics of flying insects populations controlled by large scale information. *Theor. Popul. Biol.* **2005**, *68*, 91–104. [CrossRef] [PubMed]

16. Tran, A.; Raffy, M. On the dynamics of dengue epidemics from large-scale information. *Theor. Popul. Biol.* **2006**, *69*, 3–12. [CrossRef]

17. Dumont, Y. Modeling mosquito distribution. Impact of the landscape. In *AIP Conference Proceedings*; American Institute of Physics: College Park, MD, USA, 2011; Volume 1389, pp. 1244–1247.

18. Dumont, Y.; Dufourd, C. November. Spatio-temporal Modeling of Mosquito Distribution. In *AIP Conference Proceedings*; American Institute of Physics: College Park, MD, USA, 2011; Volume 1404, pp. 162–167.

19. Umar, M.; Raja, M.A.Z.; Sabir, Z.; Alwabli, A.S.; Shoaib, M. A stochastic computational intelligent solver for numerical treatment of mosquito dispersal model in a heterogeneous environment. *Eur. Phys. J. Plus* **2020**, *135*, 565. [CrossRef]

20. Nisar, K.; Sabir, Z.; Raja, M.Z.; Ibrahim, A.A.; Rodrigues, J.; Khan, A.S.; Gupta, M.; Kamal, A.; Rawat, D. Evolutionary Integrated Heuristic with Gudermannian Neural Networks for second Kind of Lane–Emden Nonlinear Singular Models. *Appl. Sci.* **2021**, *11*, 4725. [CrossRef]

21. Ammar, M.K.; Amin, M.R.; Hassan, M. Calculation of line of site periods between two artificial satellites under the action air drag. *Appl. Math. Nonlinear Sci.* **2018**, *3*, 339–352. [CrossRef]

22. Sabir, Z.; Raja, M.A.Z.; Khalique, C.M.; Unlu, C. Neuro-evolution computing for nonlinear multi-singular system of third order Emden–Fowler equation. *Math. Comput. Simul.* **2021**, *185*, 799–812. [CrossRef]

23. Boykov, I.; Roudnev, V.; Boykova, A. Stability of Solutions to Systems of Nonlinear Differential Equations with Discontinuous Right-Hand Sides: Applications to Hopfield Artificial Neural Networks. *Mathematics* **2022**, *10*, 1524. [CrossRef]

24. Ammar, M.K.; Amin, M.R.; Hassan, M. Visibility intervals between two artificial satellites under the action of Earth oblateness. *Appl. Math. Nonlinear Sci.* **2018**, *3*, 353–374. [CrossRef]

25. Khodadadian, A.; Parvizi, M.; Teshnehlab, M.; Heitzinger, C. Rational Design of Field-Effect Sensors Using Partial Differential Equations, Bayesian Inversion, and Artificial Neural Networks. *Sensors* **2022**, *22*, 4785. [CrossRef]

26. Dai, P.; Yu, X. An Artificial Neural Network Approach for Solving Space Fractional Differential Equations. *Symmetry* **2022**, *14*, 535. [CrossRef]

27. Guo, Y.; Cao, X.; Liu, B.; Gao, M. Solving partial differential equations using deep learning and physical constraints. *Appl. Sci.* **2020**, *10*, 5917. [CrossRef]

28. Umar, M.; Sabir, Z.; Raja, M.; Shoaib, M.; Gupta, M.; Sánchez, Y. A Stochastic Intelligent Computing with Neuro-Evolution Heuristics for Nonlinear SITR System of Novel COVID-19 Dynamics. *Symmetry* **2020**, *12*, 1628. [CrossRef]

29. Sabir, Z.; Umar, M.; Guirao, J.L.G.; Shoaib, M.; Raja, M.A.Z. Integrated intelligent computing paradigm for nonlinear multi-singular third-order Emden–Fowler equation. *Neural Comput. Appl.* **2021**, *33*, 3417–3436. [CrossRef]

30. Sabir, Z.; Raja, M.A.Z.; Umar, M.; Shoaib, M. Design of neuro-swarming-based heuristics to solve the third-order nonlinear multi-singular Emden–Fowler equation. *Eur. Phys. J. Plus* **2020**, *135*, 410. [CrossRef]

31. Li, Y.; Xu, L.; Ying, S. DWNN: Deep Wavelet Neural Network for Solving Partial Differential Equations. *Mathematics* **2022**, *10*, 1976. [CrossRef]

32. Agarwal, R.; Hristova, S.; O'Regan, D. Global Mittag—Leffler Synchronization for Neural Networks Modeled by Impulsive Caputo Fractional Differential Equations with Distributed Delays. *Symmetry* **2018**, *10*, 473. [CrossRef]

33. Akhmet, M.; Aruğaslan Çinçin, D.; Tleubergenova, M.; Nugayeva, Z. Unpredictable oscillations for Hopfield-type neural networks with delayed and advanced arguments. *Mathematics* **2021**, *9*, 571. [CrossRef]

34. Khan, N.A.; Sulaiman, M.; Tavera Romero, C.A.; Alarfaj, F.K. Theoretical analysis on absorption of carbon dioxide (CO2) into solutions of phenyl glycidyl ether (PGE) using nonlinear autoregressive exogenous neural networks. *Molecules* **2021**, *26*, 6041. [CrossRef] [PubMed]

35. Cheng, C.; Zhang, G.T. Deep learning method based on physics informed neural network with resnet block for solving fluid flow problems. *Water* **2021**, *13*, 423. [CrossRef]

36. Ilhan, E.; Kıymaz, I.O. A generalization of truncated M-fractional derivative and applications to fractional differential equations. *Appl. Math. Nonlinear Sci.* **2020**, *5*, 171–188. [CrossRef]

37. Baskonus, H.M.; Bulut, H.; Sulaiman, T.A. New complex hyperbolic structures to the lonngren-wave equation by using sine-gordon expansion method. *Appl. Math. Nonlinear Sci.* **2019**, *4*, 141–150. [CrossRef]
38. Vajravelu, K.; Sreenadh, S.; Saravana, R. Influence of velocity slip and temperature jump conditions on the peristaltic flow of a Jeffrey fluid in contact with a Newtonian fluid. *Appl. Math. Nonlinear Sci.* **2017**, *2*, 429–442. [CrossRef]
39. Pérez-García, V.M.; Fitzpatrick, S.; Pérez-Romasanta, L.A.; Pesic, M.; Schucht, P.; Arana, E.; Sánchez-Gómez, P. Applied mathematics and nonlinear sciences in the war on cancer. *Appl. Math. Nonlinear Sci.* **2016**, *1*, 423–436.
40. Selvi, M.S.M.; Rajendran, L. Application of modified wavelet and homotopy perturbation methods to nonlinear oscillation problems. *Appl. Math. Nonlinear Sci.* **2019**, *4*, 351–364.
41. Aghili, A. Complete solution for the time fractional diffusion problem with mixed boundary conditions by operational method. *Appl. Math. Nonlinear Sci.* **2021**, *6*, 9–20. [CrossRef]